Uncertainty in the projected Antarctic contribution to sea level due to internal climate variability

Justine Caillet[1], Nicolas C. Jourdain[1], Pierre Mathiot[1], Fabien Gillet-Chaulet[1], Benoit Urruty[1], Clara Burgard[1,2], Charles Amory[1,3], Christoph Kittel[1], and Mondher Chekki[1]

[1]Univ. Grenoble Alpes, CNRS, INRAE, IRD, Grenoble INP, Institut des Geosciences de l'Environnement, Grenoble, France
[2]Laboratoire d'Océanographie et du Climat, LOCEAN-IPSL, Sorbonne Université, CNRS-IRD-MNHN, Paris, France
[3]Laboratoire de Sciences du Climat et de l'Environnement, LSCE-IPSL, CEA-CNRS-UVSQ-UMR8212, Université Paris Saclay, Gif-sur-Yvette, France

Correspondence: Justine Caillet (justine.caillet@univ-grenoble-alpes.fr)

Abstract. Identifying and quantifying irreducible and reducible uncertainties in the Antarctic Ice Sheet response to future climate change is essential for guiding mitigation and adaptation policy decision. However, the impact of the irreducible internal climate variability, resulting from processes intrinsic to the climate system, remains poorly understood and quantified. Here, we characterise both the atmospheric and oceanic internal climate variability in a selection of three CMIP6 models
5 (UKESM1-0-LL, IPSL-CM6A-LR and MPI-ESM1.2-HR) and estimate their impact on the Antarctic contribution to sea level over the 21st century under the SSP2-4.5 scenario. To achieve this, we use a standalone ice-sheet model driven by the ocean through parameterised basal melting and by the atmosphere through emulated surface mass balance estimates. Internal climate variability affects the Antarctic contribution to changes in sea level until 2100 by 45% to 93% depending on the CMIP6 model. This may be a low estimate as the internal climate variability in the CMIP models is likely underestimated. For all the
10 three climate models and for most Antarctic regions, the effect of atmospheric internal climate variability on the surface mass balance overwhelms the effect of oceanic internal climate variability on the dynamical ice-sheet mass loss by more than a factor of 3. The atmospheric internal climate variability is similar in the three CMIP6 models analysed in this study. Conversely, the amplitude of oceanic internal climate variability around Antarctica strongly depends on the climate model as underestimated convection, due to either biases in the sea-ice behaviour or in the ocean stratification, leads to weak mid-depth ocean variability.
15 We then issue recommendations for future ice-sheet projections: use several members in the run and in its initialisation, favor 50-year averages to correct or weight simulations over the present-day period, and couple ice-sheet and climate models.

1 Introduction

The Antarctic Ice Sheet (AIS) is losing mass at an increasing rate (Rignot et al., 2019; Shepherd et al., 2019), particularly in the Amundsen and Totten/Moscow sectors, where ocean-induced melting under floating ice shelves is relatively high (Jenkins
20 et al., 2018; Hirano et al., 2023). The AIS response to future climate change, including its potential instability (Garbe et al., 2020; Armstrong McKay et al., 2022), is one of the major sources of uncertainty in projections of global sea level rise (Fox-

Kemper et al., 2021), with an estimated contribution over 2015–2100 ranging from -5 to 43 cm under a high-end anthropogenic emission scenario (ISMIP6, Edwards et al., 2021).

The AIS contribution to future sea level rise is currently mostly based on standalone ice-sheet models, forced by atmospheric
25 and oceanic data from the Climate Model Intercomparison Project (CMIP, Eyring et al., 2016). The diversity of climate conditions across the CMIP models explains an important part of the uncertainty in some of the drainage basins (Seroussi et al., 2023), despite the use of an anomaly method to reduce known biases in the CMIP models (Jourdain et al., 2020; Purich and England, 2021). Internal climate variability is usually not accounted for in the uncertainty on AIS projections. A single study, so far, has estimated that this uncertainty could be 18-21% higher due to internal climate variability (Tsai et al., 2020). This
30 was estimated using a single ice-sheet model and two versions of the same climate model.

Climate variability is the combination of two components, the variability resulting on the one hand from external forcing of both natural (e.g., volcanoes or solar activity) and anthropogenic (e.g., CO_2 emissions) sources, and internal variability on the other hand. The latter results from processes intrinsic to the climate system, due to the chaotic nature of fluid dynamics and to non-linearities in the coupled interactions between the ocean, atmosphere, land and cryosphere (e.g., Kravtsov et al.,
35 2007; Penduff et al., 2018; Gwyther et al., 2018; Hogg et al., 2022). For a given climate model, the impact of internal climate variability can be isolated by considering several forced simulations with identical external forcing but slightly different initial conditions. For this reason, an increasing number of CMIP models include several members which differ only in their initial state.

A part of the internal climate variability can be characterised as modes such as the El Niño/Southern Oscillation (ENSO)
40 and Interdecadal Pacific Oscillation (IPO), which have remote connections with the Amundsen Sea Low (ASL, Holland et al., 2022; Dalaiden et al., 2023). The ASL is a low-pressure system located over the South Pacific sector of the Southern Ocean, which generates decadal wind anomalies that affect the oceanic undercurrent along the continental slope, thereby modulating the amount of warm water flowing towards the ice shelves of the Amundsen Sea Embayment (Silvano et al., 2022). The regional influence of these modes makes internal climate variability particularly strong in the Amundsen sector: internal climate
45 variability is thought to be responsible for the retreat of Pine Island's grounding line in the 1940s (Holland et al., 2022), and mid-depth ocean warming trends over the 21st century can vary by a factor of two depending on the phasing of internal climate variability (Naughten et al., 2023).

In this paper, we first investigate atmospheric and oceanic internal climate variability of several CMIP6 models. Then, using a standalone ice-sheet model forced by CMIP6 model outputs, we quantify the impact of internal climate variability on Sea
50 Level Contribution (SLC) over the 21st century under the medium SSP2-4.5 scenario for both the whole ice sheet and the main basins, especially the Amundsen basin which is expected to be particularly affected by internal climate variability.

2 Methods

2.1 CMIP6 model selection

We choose to analyse three CMIP6 models to get a more general picture of the internal climate variability than using a single
55 model. These three models were selected both for the size of their ensemble and for their representation of the present-day
Southern Ocean and Antarctic seas, as basal melting is one of the main driver of the Antarctic contribution to sea level rise.
The selection was done based on a review of three studies:

- the evaluation of the properties of Antarctic Shelf Bottom Water (ASBW) on the continental shelf and of Circumpolar
  Deep Water (CDW), located further offshore in the Antarctic circumpolar region and expected to intrude more on the
60   continental shelf in a warmer climate, conducted by Purich and England (2021),

- the evaluation of dynamical features known to be important for the Southern Ocean, including the transport of the Antarc-
  tic Circumpolar Current (ACC), zonal wind stress properties, and meridional gradients of ocean properties, conducted
  by Beadling et al. (2020),

- the evaluation of the bottom properties of the Southern Ocean, conducted by Heuzé (2021).

65 A summary of this assessment is provided in Fig. 1. The selected models are: UKESM1-0-LL (19 members, Sellar et al., 2020),
which is among the best models in the three studies; IPSL-CM6A-LR (33 members, Boucher et al., 2020), which represents
reasonably well the deep ocean properties and to a lesser extent the main Southern Ocean dynamics, but produces overly cold
CDWs; MPI-ESM1.2-HR (10 members, Müller et al., 2018), which was evaluated in only one of the three aforementioned
studies, but has a higher ocean resolution (0.4° vs 1°) and a lower Equilibrium Climate Sensitivity (3.0°C vs 5.3 and 4.6°C,
70 Meehl et al., 2020) than the two other models. It is also interesting to note that both UKESM1-0-LL and IPSL-CM6A-LR
have some kind of prescribed ice-shelf melting at depth to ensure the conservation of the ice-sheet mass over the pre-industrial
or the entire simulation, which is known to be important for coastal ocean properties around Antarctica (Mathiot et al., 2017;
Donat-Magnin et al., 2021).

Moreover, the present-day properties of the atmosphere of the three selected CMIP6 models compare well to ERA5. Ac-
75 cording to the evaluation of the CMIP5/6 models conducted in Agosta et al. (2022), UKESM1-0-LL and MPI-ESM1.2-HR are
among the best performing models in the Antarctic region, while the IPSL-CM6A-LR model is between the first and second
quartile.

2.2 Ice-sheet model

We use the version v9.0 of the Elmer/Ice finite element model (Gagliardini et al., 2013), in a configuration of the entire Antarctic
80 Ice Sheet adapted from Hill et al. (2023). The ice dynamics is computed by solving the Shallow Shelf Approximation (SSA)
of the Stokes equations (MacAyeal, 1989), assuming an isotropic rheology following Glen's flow law (Glen, 1955) and a linear
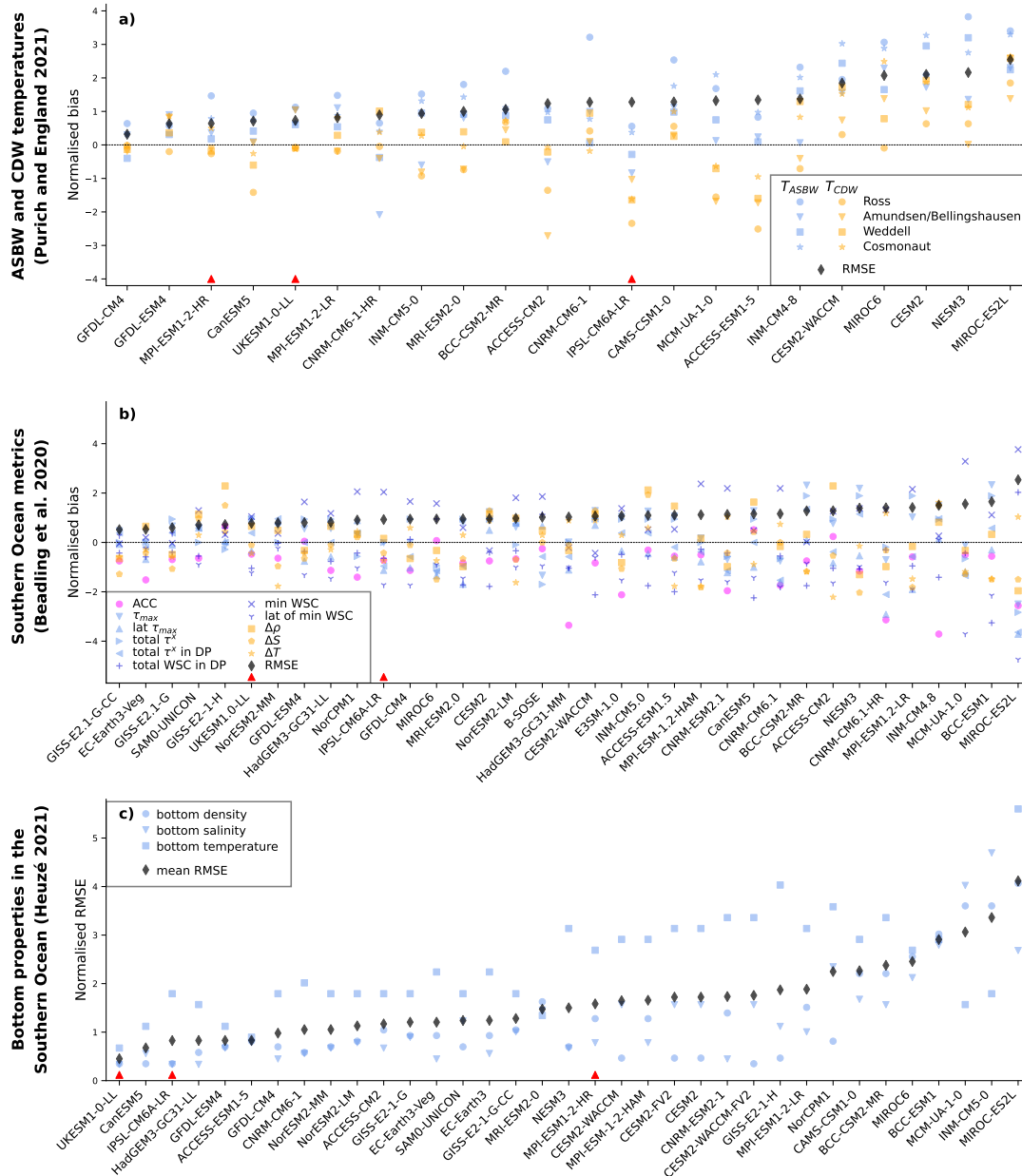
Figure 1. Assessment of Southern Ocean and Antarctic seas properties in the CMIP6 models. In each panel, CMIP models are ranked by increasing RMSE. (a) Antarctic Shelf Bottom Water (ASBW) and Circumpolar Deep Water (CDW) temperature biases in the Ross, Amundsen/Bellingshausen, Weddell and Cosmonauts seas (Purich and England, 2021, their Fig. S16). (b) Biases in the Southern Ocean metrics defined in Tab. 1 of Beadling et al. (2020) and describing several characteristics of the Antarctic Circumpolar Current, zonal wind stress strength, location and curl, as well as meridional gradients of water mass properties. (c) RMSE of bottom ocean properties (density, salinity and temperature) in the Southern Ocean (Heuzé, 2021, their Figs. 1, A1, A2). For each panel, the metric is normalised by the CMIP6 multi-model standard deviation. A red triangle indicates the selected models.

friction law. The location of the grounding line is determined using a flotation criterion and a sub-grid scheme is applied for the friction in partially floating elements (SEP3 in Seroussi et al., 2014).

The mesh is preferentially refined both close to the grounding line and in areas where observed surface velocities and thickness show high curvatures, with a maximum size of 50 km in the very interior of the ice sheet and a minimum size of 1 km in the refined areas. The model domain does not change over time, but the ice thickness is subject to a lower limit of 1 m and elements that reach this limit are considered deglaciated in the post-processing. For stability reasons, the domain boundary is slightly smoothed and isolated icebergs (ice-covered area disconnected from the ice sheet) with less than 7 elements, are removed if they appear during the simulation (i.e, their thickness is set to the critical thickness of 1 m). Apart from these corrections, we assume a steady calving front.

Inverse methods (Gillet-Chaulet et al., 2012; Brondex et al., 2019) provide viscosity and friction parameters by minimising the misfit between modelled and observed velocities from Mouginot et al. (2019) using the ice thickness from BedMachine-Antarctica-v2 (Morlighem et al., 2020). Details of the inversion are available in Hill et al. (2023). Our model configuration does not represent a prognostic evolution of ice temperature and damage that may affect viscosity in transient simulations. From the inversion step, we run a 20-year "relaxation" under the present-day forcing described hereafter. This attenuates the artificial high surface elevation rate of change that occurs when we switch from a diagnostic to a prognostic simulation (Gillet-Chaulet et al., 2012).

The PICO box model (Reese et al., 2018) is used to parameterise ice-shelf basal melting, with a distinct calibration from Hill et al. (2023). Here, the parameters are those detailed in Reese et al. (2023), i.e., $C = 2\,\mathrm{Sv\,m^3\,kg^{-1}}$ and $\gamma_T = 5.5 \times 10^{-5}\,\mathrm{m\,s^{-1}}$. The present-day sea floor temperature and salinity for each of the 19 regions defined in Reese et al. (2018) are extracted from the ISMIP6 ocean climatology (Jourdain et al., 2020) and averaged within 50 km of the ice-shelf front as described in Burgard et al. (2022). A correction of temperature, ranging from -1.8°C to 0.6°C with respect to the ocean climatology, is added to match the 1994-2018 melt rates estimates from Adusumilli et al. (2020) (see Fig. 2).

The present-day Surface Mass Balance (SMB) is based on the 1995-2014 climatology (a period of relatively stable SMB) of the RACMO-2.3.p2 regional climate model (Van Wessem et al., 2018). In contrast to Hill et al. (2023), we do not correct the surface mass balance, but we apply a 10% reduction of the inverted friction coefficients to be closer to the observed ice-sheet mass change (The IMBIE Team, 2018) for both West and East Antarctica. Our configuration correctly estimates the mass loss trend in the West Antarctica but still overestimates mass gain trend in East Antarctica and in the Peninsula (Tab. 1). This mass change trend bias is quite common in ice-sheet models (Seroussi et al., 2020; Aschwanden et al., 2021). This is why our results are primarily analysed in relative terms.

2.3 Ice-sheet projections to 2100

Antarctic future mass change results from combined effects of surface mass balance and dynamics changes. Given that variations in surface mass balance have little impact on the dynamical contribution over a century (Seroussi et al., 2014, 2023), these two contributions can be analysed separately, then summed to reconstruct the combined effect (Bindschadler et al., 2013).
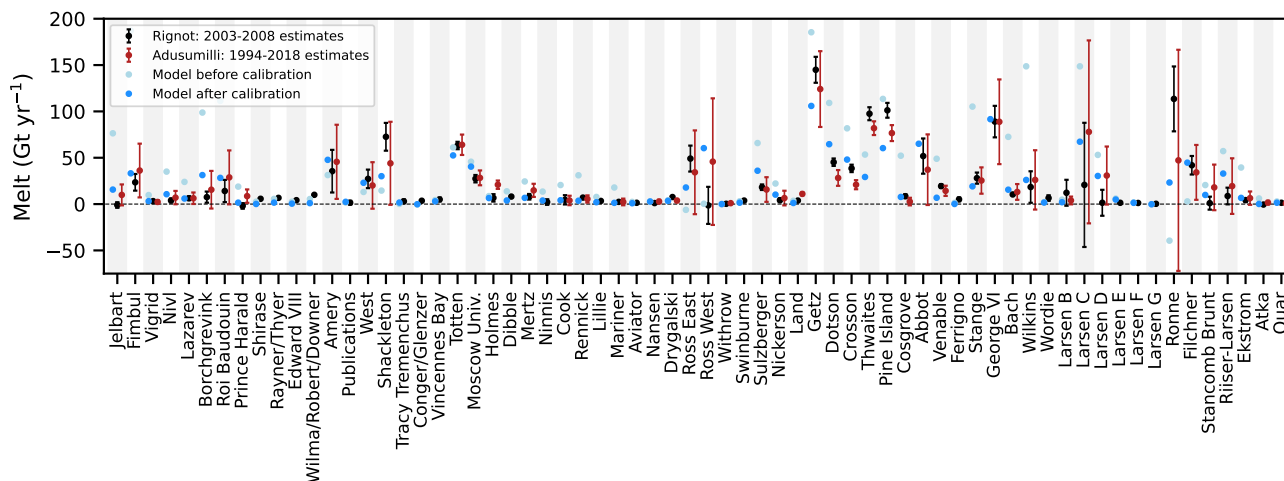
Figure 2. Basal melt rate of main ice shelves over the period 1994-2014 before (lightblue) and after calibration (blue) compared to the melting estimates over the period 1994-2018 from Adusumilli et al. (2020, in red). Observed data uncertainties correspond to one standard deviation. Note that the data from Adusumilli et al. (2020) only cover the area northward of 81.5°S, which excludes part of the Filchner-Ronne and Ross ice shelves. Melting estimates over the period 2003-2008 from Rignot et al. (2013, in black) are shown for comparison.

Table 1. Rates of ice-sheet mass change ($Gt\,yr^{-1}$) for the entire Antarctica (AIS) and the main areas of East Antarctica (EAIS), West Antarctica (WAIS) and Peninsula (APIS).

	IMBIE estimates (1992-2017)	Elmer/Ice (1994-2014)
AIS	-109±56	+36
EAIS	+5±46	+107
WAIS	-94±27	-127
APIS	-20±15	+35

To investigate the impact of oceanic internal climate variability on the Antarctic Ice Sheet projections, we run Elmer/Ice simulations constrained by the ocean of several members of the selected CMIP models from 2015 to 2100. We use the medium SSP2-4.5 scenario, which corresponds to a global warming of 1.4 to 3.0°C from 1995-2014 to 2081-2100 (90% confidence interval, Lee et al., 2021). Because of the numerical cost of our simulations, we select a limited number of members. The selection is made over the current period (1995-2014 means) to cover the widest range of values for both the ocean temperature on the continental shelf in the Amundsen Sea and the SMB over the whole of Antarctica (see next section). In total, we run 11 simulations, five with the IPSL-CM6A-LR model (r1i1p1f1, r3i1p1f1 , r6i1p1f1, r11i1p1f1, r25i1p1f1), four with the UKESM1-0-LL model (r1i1p1f2, r2i1p1f2, r4i1p1f2, r8i1p1f2) and two with the MPI-ESM1.2-HR model (r1i1p1f2, r2i1p1f2).

All the Elmer/Ice simulations start from the same state, corresponding to 2014, and yearly anomalies are added to the present-day forcing to drive future projections as previously done in ISMIP6 (Nowicki et al., 2020). All the anomalies are

125 calculated with respect to the 1995-2014 period of a given member.

The annual ocean potential temperature and practical salinity from CMIP model outputs were interpolated to a stereographic (8 km × 8 km × 60 m) grid, then extrapolated to fill unrepresented areas as in Jourdain et al. (2020). The corresponding ocean anomalies were then added to the present-day temperature and salinity to feed the ice-shelf basal melt parameterisation.

Regional climate projections were not used to calculate the future SMB of ISMIP6-Antarctica (Nowicki et al., 2020; Seroussi

130 et al., 2020), mostly because they were not available early enough in the intercomparison process. Since then, this kind of simulations have been used to refine SMB projections (Kittel et al., 2021, 2022). Using a dedicated regional climate model is particularly important for the IPSL-CM6A-LR model given that its snow physics over ice sheets is too simple to simulate firn saturation and runoff in a warmer climate. However, running the regional climate model driven by many members of the CMIP ensemble would be computationally too expensive and practically not feasible due to the non availability of 6-hourly output

135 for most members, which are needed to constrain the regional model.

In this paper, we therefore use the approach developed by Jourdain et al. (2024) to emulate the behaviour of the *Modèle Atmosphérique Régional* (MAR, Kittel et al., 2021). This method uses exponential fits of accumulation and melting perturbations due to changes in surface air temperature, as well as simple physical relationships to derive runoff and SMB. The fit parameters are calculated from 1980-2100 MAR simulations forced by the corresponding CMIP model (either IPSL-CM6A-

140 LR, UKESM1-0-LL or MPI-ESM1.2-HR). The SMB of a given member is estimated from the relevant MAR simulation of the first member, perturbed as a function of the annual temperature difference between the two CMIP model members. This method is thoroughly evaluated in Jourdain et al. (2024) for the emulation of other CMIP models and scenarios, and here we apply it to emulate other members. Similarly to the ocean forcing, we calculate annual anomalies (with respect to 1995-2014 mean SMB) and add them to the present-day SMB.

145 3 Results

We first characterize internal climate variability of the oceanic (subsect. 3.1) and atmospheric (subsect. 3.2) components in the selected CMIP6 models. For this, we use all available members and we describe the effect of internal climate variability on the present-day mean state, i.e., 1995-2014, which is used as a reference for the calculation of anomalies in ISMIP6 and in our Elmer/Ice simulations. Then, we estimate the importance of internal climate variability for sea level projections by examining

150 transient Elmer/Ice simulations from 2015 to 2100, driven by a subset of the CMIP6 ensemble used in the two first subsections (subsec. 3.3).

3.1 Oceanic internal climate variability

Oceanic internal climate variability at mid-depth is much weaker in MPI-ESM1.2-HR than in IPSL-CM6A-LR and UKESM1-0-LL (Fig. 3). MPI-ESM1.2-HR shows a relatively low and homogeneous internal climate variability on the continental shelf,

155 with typical standard deviations of 0.017 g kg^{-1} and 0.06°C across the members (Fig. 3a,d). The mean salinity of this model is too low over the whole continental shelf (34.2 g kg^{-1}) compared to the World Ocean Atlas dataset (WOA 2018 Boyer et al., 2018), particularly in front of the Ross and Filchner ice shelves (Fig. 4a,b). This suggests that the weak internal climate variability is related to an underestimation of dense water formation (Fig. 4b).

For IPSL-CM6A-LR and UKESM1-0-LL, salinity exhibits higher variability over the whole shelf (around 0.030 g kg^{-1} in

160 Fig. 3b,c) but this does not systematically lead to a high variability in temperature (Fig. 3e,f). The part that undergoes the largest variability in mid-depth temperatures in both IPSL-CM6A-LR and UKESM1-0-LL is the region extending westward from the Bellingshausen Sea to the western Ross Sea. There are nonetheless noticeable differences between the two models.

For IPSL-CM6A-LR, the largest variability in mid-depth salinity is found in the western part of the Ross Sea, where High Salinity Shelf Water (HSSW) is formed (Fig. 3b). As described by Mathiot and Jourdain (2023) and Siahaan et al. (2022), lower

165 rates of HSSW formation in the eastern Ross Sea can favor the intrusion of Circumpolar Deep Water (CDW) in the western part, which may explain why mid-depth temperature variability is highest there (Fig. 3e). In contrast, the high variability in salinity at the HSSW formation site of the eastern Weddell Sea (Fig. 3b) is probably too weak to be associated with any CDW intrusion (Fig. 3e). For UKESM1-0-LL, the highest variability in mid-depth salinity is located around Prydz Bay in East Antarctica (Fig. 3c), which is an area of important dense shelf water formation (Williams et al., 2016). It nonetheless does not induce a

170 strong temperature variability near the ice shelves (Fig. 3f). An interesting feature of UKESM1-0-LL (and IPSL-CM6A-LR to a lower extent) is the high salinity variability in the deep ocean, northward of the Amundsen Sea (Fig. 3c), which coincides with a region of high variability of sea-ice concentration (not shown) and air temperature (Fig. 5f).

We now examine the Amundsen Sea more closely as the region is particularly important for the ice-sheet mass loss. In MPI-ESM1.2-HR, the first 100 m are much fresher than observed and than in the two other models (Fig. 3g), and the entire

175 water column is too warm with an overly strong and shallow thermocline (Fig. 3j). Sea-ice concentration is considerably lower than for the other two models and observations (Fig. 4i-l), which results in a lack of deep convection on the shelf. The low oceanic internal climate variability in MPI-ESM1.2-HR may result from this lack of convection as internal climate variability in the atmosphere does not easily propagate into the deep ocean.

Both IPSL-CM6A-LR and UKESM1-0-LL seem to be prone to convection, with more realistic temperature profiles than

180 MPI-ESM1.2-HR in the Amundsen Sea. All the IPSL-CM6A-LR members are nonetheless cold biased at depth (weakest bias of -0.75°C at 900 m depth in Fig. 3k), while all the UKESM1-0-LL members are warm biased (weakest bias of +0.54°C at 900 m depth in Fig. 3l). The spread across the ensemble is large for both models, with 0.79°C (IPSL-CM6A-LR) and 0.39°C (UKESM1-0-LL) difference in the 1995-2014 mean temperature at 900 m between the extreme members.

These conclusions remain valid for 60-year averages instead of 20-year averages, albeit with attenuated internal climate

185 variability. For example, there is still 0.43°C (IPSL-CM6A-LR) and 0.34°C (UKESM1-0-LL) difference in the 1955-2014 mean temperature at 900 m between the extreme members (not shown). This finding is consistent with a strong internal climate variability at multi-decadal time scales in the Amundsen Sea, as previously pointed out by Purich and England (2021) who identified typical periodicity of approximately 30 years for MPI-ESM1.2-HR, 70 years for IPSL-CM6A-LR and 120 years for

UKESM1-0-LL (their Fig. S6). In comparison, paleoclimate reconstructions indicate a ∼50-year period for the wind variability

190   at the Amundsen Sea shelf break (Holland et al., 2022).

3.2   Atmospheric internal climate variability

The SMB is defined as the difference between precipitation (liquid and solid, positive contribution) and evaporation, sublimation and run-off (negative contribution). The present-day Antarctic SMB mostly consists of snowfall, a small part of which (<10%) is sublimated at the surface and in blowing snow (Van Wessem et al., 2018; Agosta et al., 2019; Mottram et al., 2021).

195   Run-off is currently negligible as most of the meltwater refreezes due to cold temperatures. By 2100 and for the SSP2-4.5 medium scenario, run-off is supposed to remain limited (Kittel et al., 2021), so the SMB is projected to increase largely due to the increased water vapour saturation in warmer air (e.g. Krinner et al., 2008; Agosta et al., 2013). Here, we therefore focus on SMB, precipitations and air temperatures.

In contrast to the ocean, the atmospheric internal climate variability is relatively similar in the three selected CMIP6 models

200   (Fig. 5). This is partly due to similar present-day SMB: the integrated value over the whole ice sheet ranges between 2641 and 2892 $\mathrm{Gt\,yr^{-1}}$ for all members of the three models. The present-day SMB internal climate variability is stronger in coastal regions (Fig. 5a-c) where the average SMB is higher (not shown), consistently with the precipitation variability in the CMIP simulations (Fig. 5g-i). The largest SMB internal climate variability is simulated along the coast of the Amundsen and Bellingshausen seas, which is due both to the particularly high present-day mean SMB and to the high internal climate variability of

205   atmospheric circulation and air temperature in these regions (Fig. 5d-i). As previously reported by Marshall and Thompson (2016), the internal climate variability of sea level pressure and air temperature have the typical characteristics of the two Pacific-South American modes (usually referred to as PSA1 and PSA2), which are associated with wave trains originating in the tropical Pacific and possibly modulated by feedbacks with clouds and sea-ice (Wang et al., 2022).

3.3   Impact of internal climate variability on the Antarctic contribution to sea level

210   In our ice-sheet projections, Antarctica gains mass over the century for all members of the three CMIP models, with an estimated SLC in 2100 ranging from -1.34 to -8.46 cm (Fig. 6a). This contribution results from a compensation between (*i*) increased ice mass flux through the grounding line forced by the ocean (Fig. 6b), mainly occurring in West Antarctica (Fig. 6h) and (*ii*) increasing SMB (Fig. 6c), occurring in each region (Fig. 6f,i,l). Regions behave in different ways. While the East Antarctica and the Peninsula gain mass (SLC in 2100 ranging respectively from -3.80 to -6.32 cm in Fig. 6d and from

215   -0.96 to -2.24 cm in Fig. 6j), West Antarctica looses mass (SLC in 2100 ranging from +0.11 to +3.78 cm in Fig. 6g). The West Antarctic positive SLC is mostly explained by Pine Island and Thwaites ice shelves (∼3 cm in Fig. 7c, basin 11) as well as Getz ice shelf (∼1 cm, basin 10). The absolute trends in East Antarctica and the Peninsula regions are largely contaminated by the unforced drift in Elmer/Ice (see section 2.2), but the simulations can still inform on the sensitivity to internal climate variability.

220   Internal climate variability affects the estimated SLC of Antarctica in 2100 by more than 45%, 79% and 93% for the IPSL, UKESM and MPI models respectively (considering the difference between the lowest and highest member divided by the
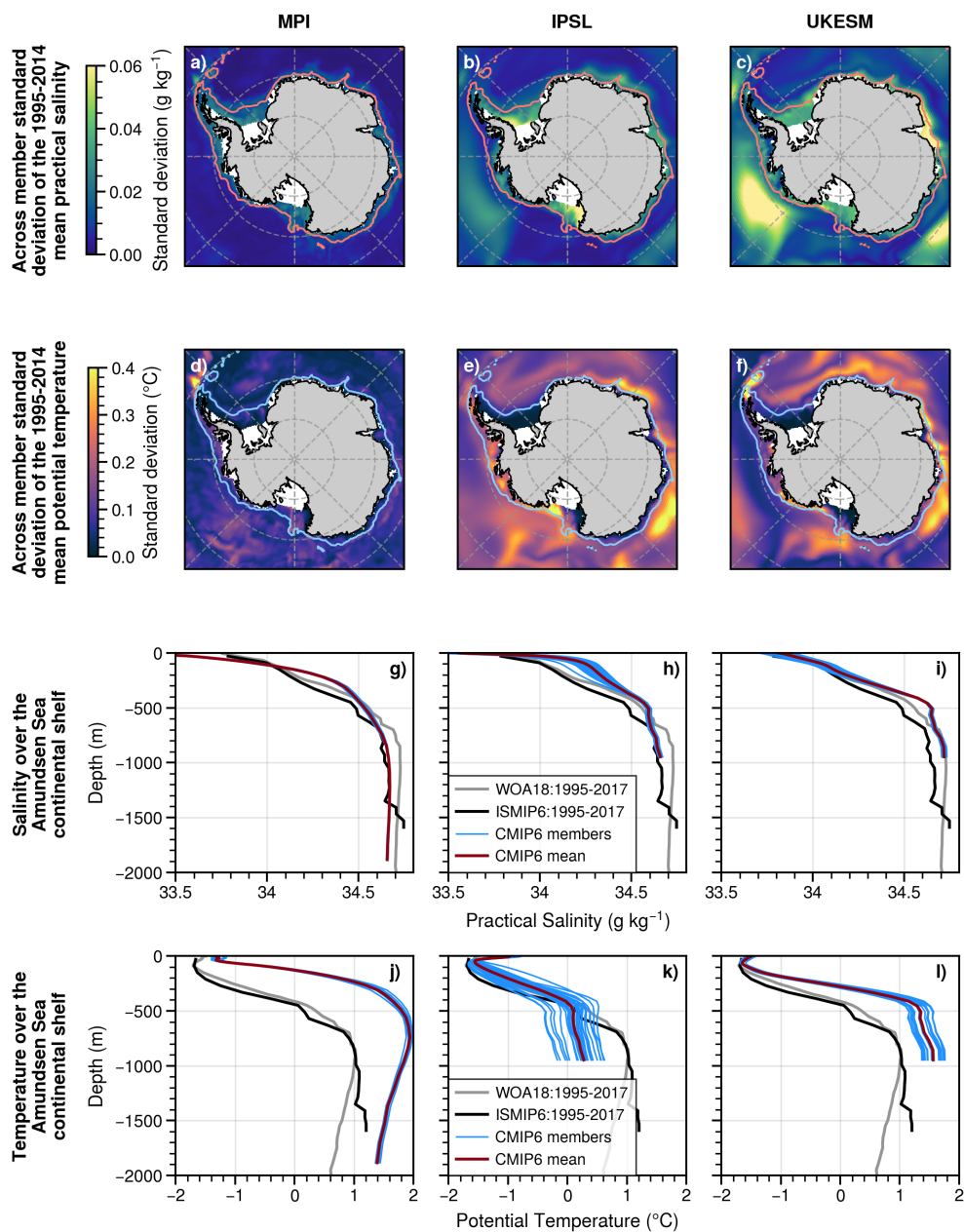
Figure 3. Comparison of the saline and thermal properties of the CMIP6 models MPI-ESM1.2-HR (left), IPSL-CM6A-LR (middle) and UKESM1-0-LL (right). (a-c) standard deviation of the 1995-2014 mean practical salinity across the ensemble relative to the multi-member mean, considering the salinity averaged from 200 m to 700 m depth. The 1500 m isobath (pink) delimits the continental shelf. (d-f) same as (a-c) but for potential temperature and with the 1500 m isobath in blue. (g-i) mean vertical profiles of practical salinity on the Amundsen Sea continental shelf (as defined in Caillet et al., 2023). For each model, the blue curves represent the individual members (1995-2014 mean), and the red line the multi-member mean. The grey curve corresponds to the 2018 World Ocean Atlas data (WOA 2018, Boyer et al., 2018) over the period 1995-2017 and the black curve to observational climatology based on the WOA, EN4 and MEOP datasets and built for ISMIP6 (Jourdain et al., 2020). (j-l) same as (g-i) but for potential temperature.
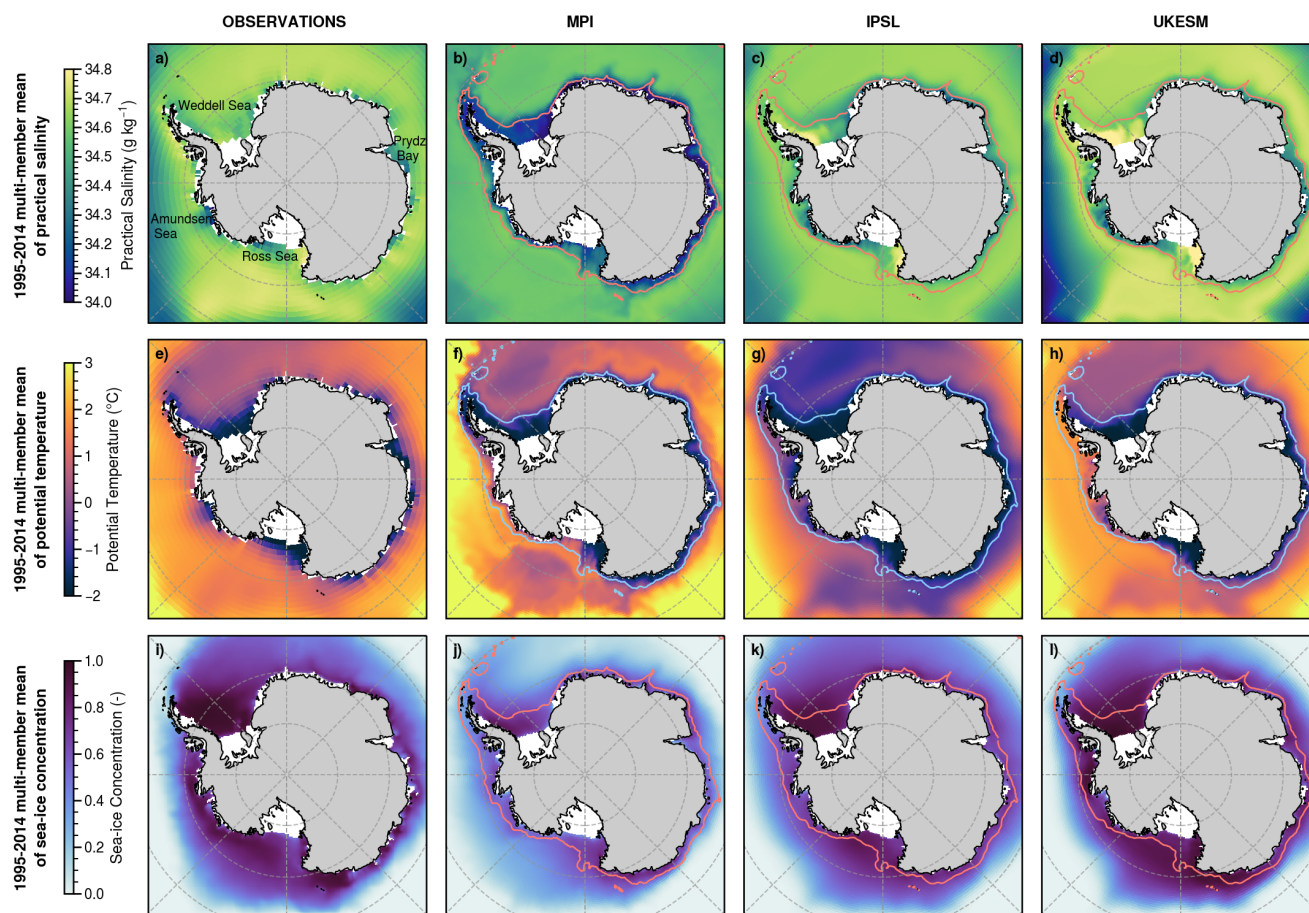
Figure 4. Comparison of the saline, thermal and sea-ice properties of observations (left) and CMIP6 models MPI-ESM1.2-HR (middle left), IPSL-CM6A-LR (middle right) and UKESM1-0-LL (right). (a) 1995-2017 mean practical salinity from the 2018 World Ocean Atlas datasets(WOA 2018, Boyer et al., 2018), considering the salinity averaged from 200 m to 700 m depth. (b-d) 1995-2014 mean practical salinity across the climate model ensemble, considering the salinity averaged from 200 m to 700 m depth. The 1500 m isobath (pink) delimits the continental shelf. (e) same as (a) but for potential temperature. (f-h) same as (b-d) but for potential temperature and with the 1500 m isobath in blue. (f) 1995-2014 mean sea-ice concentration from NSIDC dataset (version 4.0) (Comiso, 2023). (j-l) same as (b-d) but for sea-ice concentration.
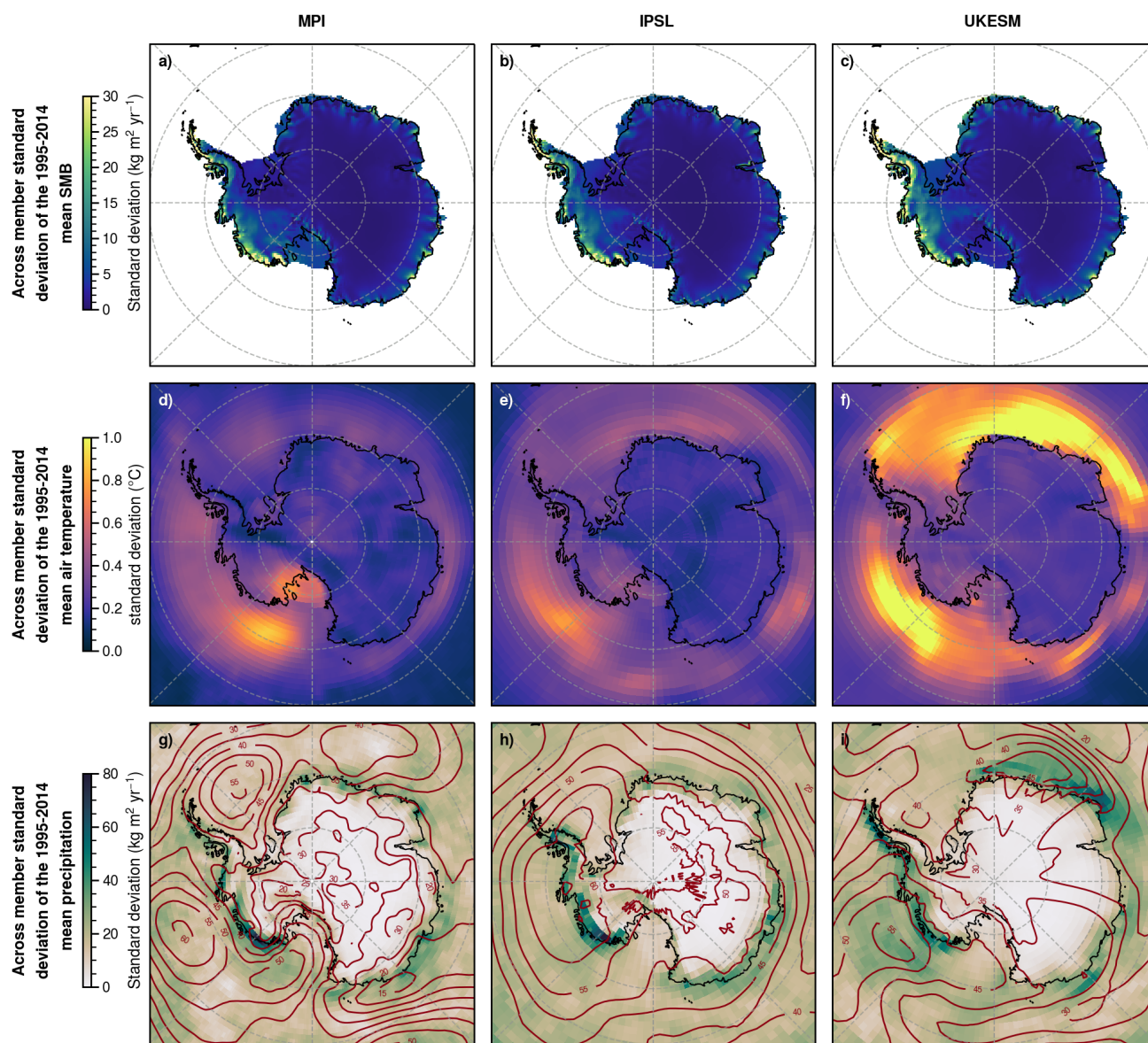
Figure 5. Comparison of the internal climate variability in surface mass balance, air temperature, precipitation and sea level pressure in MPI-ESM1.2-HR (left), IPSL-CM6A-LR (middle) and UKESM1-0-LL (right). (a-c) standard deviation of the 1995-2014 mean SMB across the ensemble relative to the multi-member mean, from the MAR-based reconstructions. (d-f) same as (a-c) but for air temperature at 2 m (directly from the CMIP6 outputs). (g-i) same as (a-c) but for total precipitation (shaded) and sea level pressure (contours every 5 hPa) from the CMIP6 outputs.

multi-member mean). Thus, the estimated SLC can vary by 1.64 cm, 4.35 cm and 2.33 cm, respectively (Fig. 6a) (considering the difference between the lowest and highest member). For the three climate models and in most Antarctic regions, the effects of atmospheric internal climate variability overwhelm the effects of oceanic internal climate variability (Figs. 6-7). This is also

225 true for West Antarctica where the SLC trend mostly results from the ocean-induced dynamics of the ice sheet but internal climate variability results from the atmosphere. On average, the amplitude of SLC variability relative to the atmosphere is 3.4 times higher than that relative to the ocean.

4   Discussion

4.1   Robustness of internal climate variability in climate models

230 Since all the diagnoses we have done are based on CMIP models, the realism of their internal climate variability needs to be addressed.

Parsons et al. (2020) compared the global mean surface air temperature of CMIP piControl simulations to paleoclimate proxies representative of the 1450-1849 period. While some of the CMIP6 models had a high-biased temperature variability, the three models used in this study are within the observational plausible range, with standard deviation (for variability beyond

235 25-year timescales) of 0.12°C in IPSL-CM6A-LR, 0.09°C in UKESM1-0-LL and 0.08°C in MPI-ESM1.2-HR.

However, based on ice core reconstructions of temperatures at the surface of Antarctica over the past 1,000 years, Casado et al. (2023) estimated that the internal climate variability was underestimated over Antarctica in the CMIP5 and CMIP6 models, although the three models used here were not part of the assessment. Previdi and Polvani (2016) suggested that the SMB interannual internal climate variability is well captured by the CMIP5 models, but this is only based on the reanalysis

240 period and is therefore more relevant for the interannual variability than for the multi-decadal variability that is emphasized in our work. The higher fidelity of the internal climate variability in CMIP models at the interannual frequency than at multi-decadal frequencies was also reported by Cheung et al. (2017) for the main modes of variability in the Atlantic and Pacific oceans.

Our results also show that the amplitude of oceanic internal climate variability around Antarctica strongly depends on

245 the climate model. The low variability of the MPI model is inconsistent with observations. This may result from a poor representation of some processes, in particular an underestimation of dense water formation and freshwater fluxes from basal melting, as well as underestimated sea ice production, which results in a lack of deep convection on the continental shelf and prevents any exchange between the mid-depth ocean and the atmosphere (see subsect. 3.1). Based on an eddy resolving 1/4° ocean model, Sérazin et al. (2017) have estimated that chaotic low-frequency oceanic internal climate variability overwhelms

250 the atmospheric forced oceanic variability in the Southern Ocean. This suggests that the multi-decadal oceanic internal climate variability of coarser resolution models, like those considered here, could be underestimated.

Furthermore, climate models do not explicitly include the ice sheet, although the non-linearities due to ice-sheet–ocean and ice-sheet–atmosphere interaction have the potential to generate internal climate variability (Kravtsov et al., 2007; Gwyther et al., 2018).
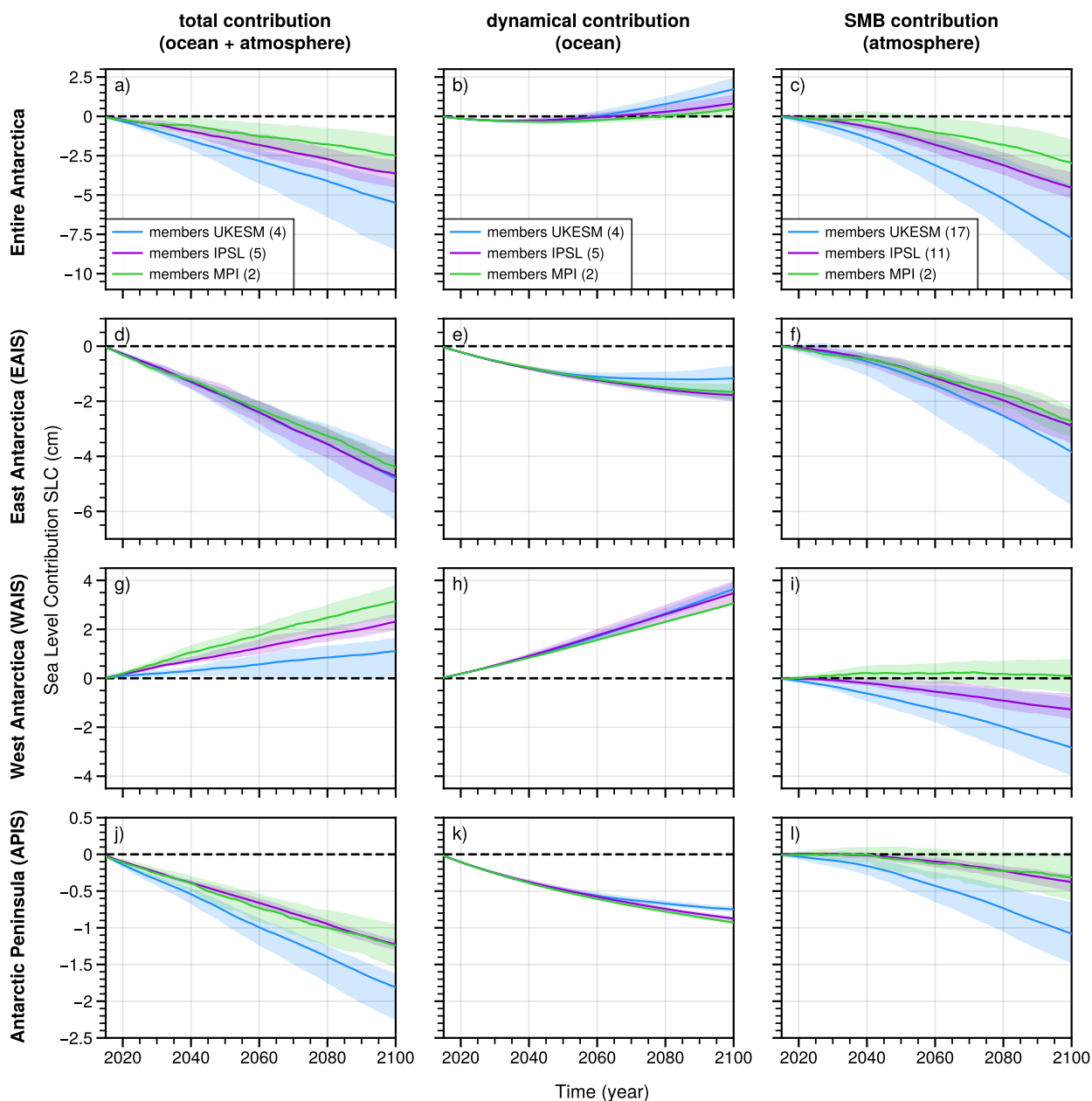
Figure 6. Antarctic Sea Level Contribution (SLC) over the 21st century relative to year 2015 under the SSP2-4.5 scenario, for MPI-ESM1.2-HR (green), IPSL-CM6A-LR (purple) and UKESM1-0-LL (blue). Results are displayed for the whole ice sheet (upper row) and for the main sub-regions (as defined in The IMBIE Team, 2018). The left rows show the combination of the dynamical ice-sheet contribution (modulated by the oceanic internal climate variability, middle row) and the surface mass balance contribution (modulated by the atmospheric internal climate variability, right row). The dynamical contribution is calculated from the change in volume above flotation minus the accumulated SMB changes, using the method described in Goelzer et al. (2020) to convert to sea level variations. The SMB contribution is calculated over the grounded ice area of BedMachine-Antarctica-v2, which is very close to Elmer/Ice's initial state (difference of less than 0.1% in grounded area). The use of the grounded ice area from BedMachine-Antarctica-v2 instead of the one from Elmer/ice (which takes into account the grounding line retreat), impacts the SLC due to the SMB by less than 1 mm.

14
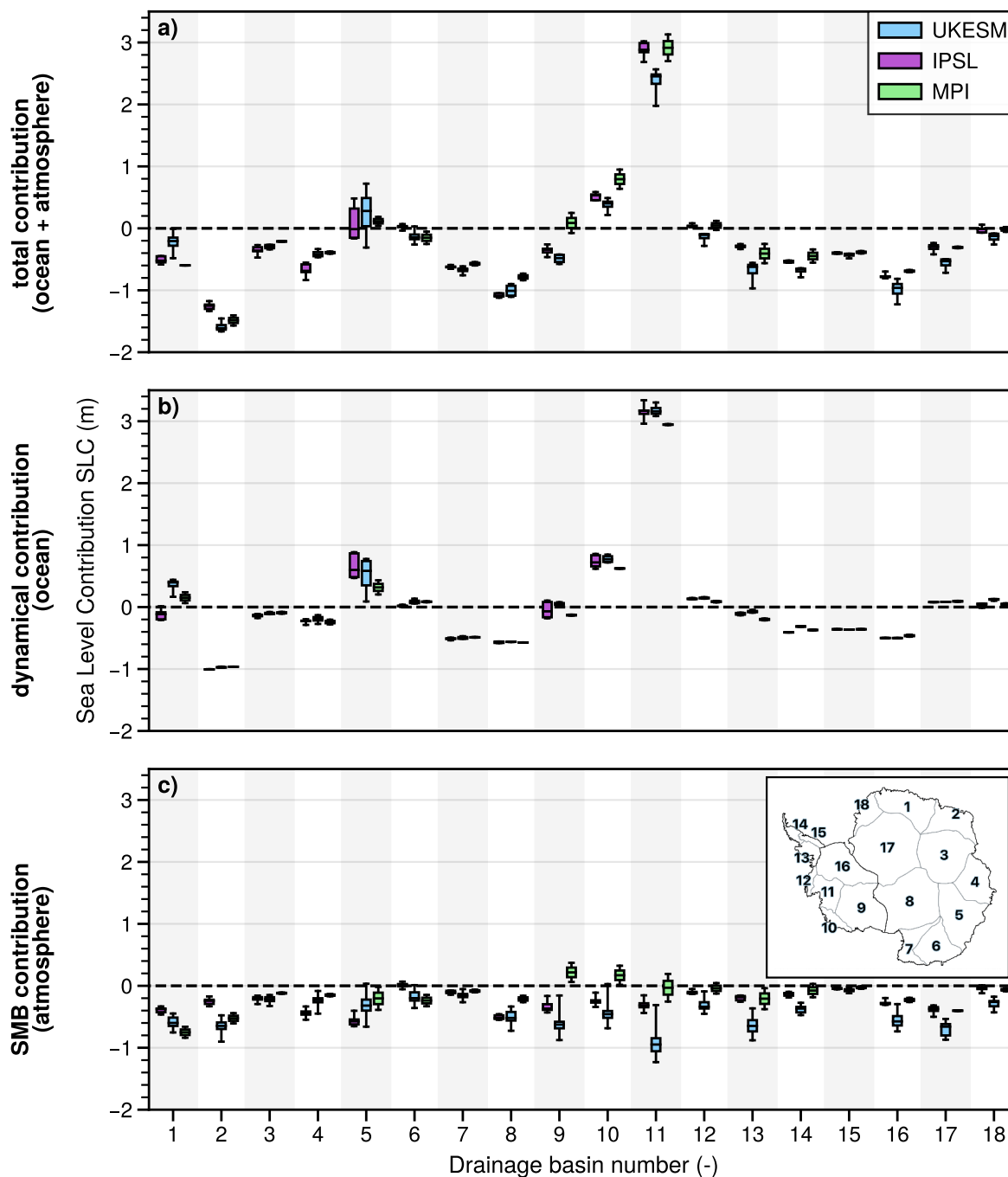
Figure 7. Regional Antarctic Sea Level Contribution (SLC) in 2100 relative to year 2015 for MPI-ESM1.2-HR (green), IPSL-CM6A-LR (purple) and UKESM1-0-LL (blue), integrated over the IMBIE drainage basins shown in (c) The IMBIE Team (2018). a) all contributions, b) dynamical ice-sheet contribution modulated by the ocean internal climate variability and d) the SMB contribution modulated by the atmospheric internal climate variability (see methods and definitions in the caption of Fig. 6). The box plots correspond to the ensemble median (line), interquartile range (box) and total range (whiskers) of each model.

255   Therefore, the low-frequency internal climate variability that affects the ice-sheet mass through oceanic and atmospheric pathways is probably underestimated in current climate models and its impact on the Antarctic SLC as well.

4.2   Internal climate variability as a source of uncertainty in sea level projections

Our simulations, involving three climate models, suggest that the choice of climate model and internal climate variability both have a similar impact on Antarctic SLC, although there are disparities on a finer scale. The relative importance of internal

260   climate variability in our simulations (45-93%) is higher than the 18-21% reported by Tsai et al. (2020). However, its absolute importance is lower in our simulations, with a 2015-2100 SLC modulated by 1.6 to 4.4 cm, versus 8 cm in Tsai et al. (2020). This is likely due to the fact that the SLC projections of Tsai et al. (30 to 48 cm) are at the very high end of the ensemble of other ice-sheet projections (Seroussi et al., 2020; Payne et al., 2021; Coulon et al., 2023), which is partly due to the parameterised ice-shelf hydrofracturing and ice cliff failure in Tsai et al. (2020) as opposed to the aforementioned other models. In contrast,

265   our simulations are towards the low end of the spectrum (-8.5 to -1.3 cm) due to the moderate scenario (SSP2-4.5), although the scenario has only a limited impact on Antarctic projections to 2100 (Seroussi et al., 2020; Fox-Kemper et al., 2021), and to the present-day drift in East Antarctica and Peninsula that we did not remove from our projected trends.

The anomaly method used to build the ocean and atmospheric forcing in both our experiments and in ISMIP6 (Nowicki et al., 2020) was designed to correct biases in SMB and ocean melting over the 1995-2014 period. However, given the high

270   variability of 20-year means, correcting a random phase of the historical CMIP simulations towards the actual 1995-2014 period may significantly shift the projections. For example, members with colder forcing over the present-day period become warmer throughout the 21st century due to the correction. Casado et al. (2023) recommend averaging over 50-years to be long enough to weaken internal climate variability and short enough not to dilute forced trends. This corresponds to the typical period of internal climate variability in the paleoclimate reconstructions (Holland et al., 2022). As discussed in subsect. 3.1,

275   some models like UKESM1-0-LL nonetheless have internal climate variability over longer periods, so that 50-year averages do not attenuate internal climate variability to a significant extent. Another issue with extending the period over which the correction is applied is that not so many observations were available 50 years ago in Antarctica.

Given the difficulties of correcting biases, it is tempting to select the members that are most in phase with observations and not applying any bias correction, which is investigated in the next subsection. It is nonetheless important to consider that

280   the anomaly method is only responsible for a part of the uncertainty associated with internal climate variability. Indeed, Tsai et al. (2020) highlighted important internal climate variability despite correcting the 1920–2012 period. As ice-sheet modellers sometimes run large ensemble simulations to select or weight the members that best fit observational records (e.g., Coulon et al., 2023), it seems important that they either consider multiple climate model members or select the more realistic ones.

4.3   Identifying the best member

285   Given the importance of internal climate variability, it is tempting to select the member that is most in phase with the observational record. We here investigate this possibility with the example of the IPSL-CM6A-LR model and its 33 members. The first challenge is to define metrics that can be used to quantify the phasing of individual members. Among the observations that are

available over several decades, it is somehow an expert judgement to decide which metrics are most relevant for the Antarctic
mass variations.

290   Here we propose to calculate the following metrics for individual members, in order to assess the complexity of identifying
a best member:

- Root mean squared difference between the multi-year mean ocean temperature profiles measured and modelled in front
of Pine Island (years 1994, 2000, 2007, 2009, 2010, 2012, as given in Dutrieux et al., 2014) and Dotson (years 2000,
2006, 2007, 2009, 2011, 2012, 2014, as given in Jenkins et al., 2018) ice shelves. This is a proxy for the phase of
295   multi-decadal variability in the region where the ocean has triggered the largest ice-sheet mass loss.

- Root mean squared difference between the standard deviation of multi-year ocean temperature profiles measured and
modelled in front of Pine Island and Dotson ice shelves. This is a proxy for the amplitude of multi-decadal variability in
the region where the ocean has triggered the largest ice-sheet mass loss.

- Difference between observed and modelled trend in the Southern Annular Mode (SAM), estimated over 1965-2014
300   based on the index defined by Marshall (2003). SAM affects both the Antarctic SMB (Medley and Thomas, 2019) and
ice-shelf basal melting (Verfaillie et al., 2022). Here we evaluate the phase of multi-decadal variability in individual
members by quantifying the modulation of the SAM 60-year trend by internal climate variability.

- Pearson correlation coefficient, root mean squared difference between and standard deviation of the observed and mod-
elled Southern Annular Mode index (SAM, Marshall, 2003) with a 5-year running window on detrend data over 1965-
305   2014. SAM index is based on the zonal pressure difference between the latitudes of 40°S an 65°S and is a proxy for the
phase and amplitude of inter-annual variability over all Antarctica as SAM has a large impact on atmospheric and oceanic
circulations. Taylor diagram combines these 3 metrics to quantify the degree of correspondence between modelled and
observed SAM.

- Pearson correlation coefficient, root mean squared difference between and standard deviation for the observed and mod-
310   elled Tripole Index for the Interdecadal Pacific Oscillation (TPI, Henley et al., 2015) with a 5-year running window over
1854-2014. The TPI is based on the difference between the Sea Surface Temperature Anomalies (SSTA) averaged over
the central equatorial Pacific and the average of the SSTA in the Northwest and Southwest Pacific. The TPI describes
decadal to interdecadal changes in the strength of the El Niño–Southern Oscillation (ENSO) and its teleconnections.
ENSO affects the West Antarctic SMB (Genthon and Cosme, 2003; Scott et al., 2019) and ice-shelf basal melting in the
315   Amundsen Sea (Steig et al., 2012; Holland et al., 2019) through the south-eastward propagation of atmospheric Rossby
waves from the inter-tropical Pacific. Taylor diagram combines these 3 metrics to quantify the degree of correspondence
between modelled and observed TPI.

- Comparison of the mean ocean temperature at 750 m depth on the continental shelf in the Amundsen Sea between iden-
tified warm periods and the preceding cold periods. Three warm periods have been identified in observations: 1945±12

320   (1933-1957), 1970±4 (1966-1974) (based on sediment records, Smith et al., 2017) and 2006-2012 (based on Dotson and
        Pine Island melt rates estimates, Dutrieux et al., 2014; Jenkins et al., 2018). These periods are compared respectively
        to 1850-1932, 1958-1965 and 1975-2005, supposed to be colder periods. For each member, we assume that the warm
        period exists if a 5-year mean, at least, within years that define the warm period is higher than the mean of the preceding
        cold period. This is a proxy for the phase of multi-decadal variability in the region where the ocean has triggered the
325   largest ice-sheet mass loss.

        – Root mean squared difference between observed and modelled sea-ice concentration trend around Antarctica over 1979-
          2014 (version 4, Meier et al., 2022). Here, we evaluate the phase of multi-decadal variability in individual members by
          quantifying the modulation of sea-ice concentration trend by internal climate variability (Zhang et al., 2019).

        – Root mean squared difference between the 1995-2014 average SMB output of the MAR simulations forced by ERA5
330   described in Kittel et al. (2021) and the reconstructed SMB of each member of the IPSL-CM6A-LR model on the same
          period as described in Jourdain et al. (2024).

    We then rank the performance of all the members by assigning them a rank, with lower rank for the member that best
matches the observations):

        – for root mean squared difference (RMSE) metric, the member with the lowest (respectively highest) RMSE value is
335   assigned rank 1 (respectively rank 33).

        – for metrics relative to Taylor Diagram (Pearson correlation coefficient and standard deviation), we first calculate a rank
          for each individual metric by assigning the lowest rank value to the lowest Pearson correlation coefficient and to the
          lowest difference between observed and modelled standard deviation. We then average all calculated ranks and finally
          assign the best (worst) final rank to the lowest (highest) average.

340   – for metric relative to warm and cold period alternation, we assume that the warm period exists if a 5-year mean, at least,
          within years that define the warm period is higher than the mean of the preceding cold period. If the condition is met,
          the member is assigned the value 1, and 0 otherwise. This process is applied to each of the three warm periods and the
          values are then summed. Members with a value of 3 (of 0) are assigned the best (the worst) rankings.

    The ranks of all members for all metrics are presented in Fig. 8. Overall, ranks are not very consistent across the chosen
345 metrics, and no member is best for all metrics. Although the perfect member does not exist, some members nevertheless seem
more in phase with the observed climate variability than the other members. We have ranked the members according to the
weighted average rank of each metric (weight of 1) (see top blue value on Fig. 8). Member 26 seems to be the most consistent
with the observed variability despite a lack of variability in front of Pine Island and a sea-ice trend that is mostly negative as
opposed to the positive observed trend.

350   However, the member selection appears very sensitive to the list of chosen metrics, and the phasing of the best member may
be only marginally better than for the other members. Given the number of degrees of freedom of climate models, it would
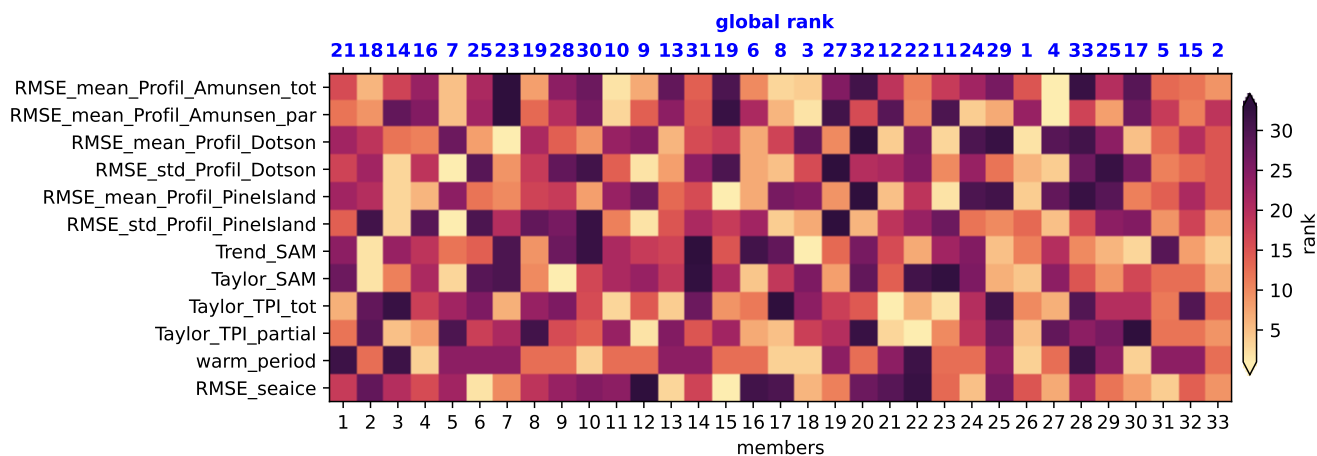
Figure 8. Combination of relevant metrics for evaluating members of the IPSL-CM6A-LR model compared to various observations/index data. The y-axis represents the selected metrics while the x-axis represents individual members. A rank of 1 (respectively 33) refers to the member with the value closest to (respectively furthest from) the assessed observational value. The blue numbers at the top indicate the member's overall ranking, with equal weight for all metrics.

probably be unrealistic to expect finding a member perfectly in phase with the observed variability among ensembles of a few tens of members, even if models were not biased. For these reasons, it appears judicious to consider several climate model members in ice-sheet projections, to account for the substantial uncertainty related to internal climate variability.

5 Conclusions

In this study, we show that internal climate variability affects the Antarctic contribution to changes in sea level until 2100 by 45%-93%, i.e., a variation between 1.6 and 4.4 cm under the SSP2-4.5 scenario. This may be a low estimate as the internal climate variability of the CMIP models is likely underestimated. In our case, the uncertainty in Antarctic sea-level contribution due to internal climate variability is of comparable magnitude as the uncertainty related to the choice of the climate model. The internal climate variability has a strong multi-decadal component, so that (i) it is not completely diluted over a century, and (ii) it strongly affects the 20-year averages used to build the forcing anomaly.

For all three climate models and for most Antarctic regions, the effect of atmospheric internal climate variability on the surface mass balance overwhelms the effect of oceanic internal climate variability on the dynamical ice-sheet mass loss by more than a factor of 3. The atmospheric internal climate variability is similar in the three CMIP6 models analysed in this study. Conversely, the amplitude of oceanic internal climate variability around Antarctica strongly depends on the climate model. The oceanic internal climate variability of the MPI-ESM1.2-HR model is very low, which may be explained by underestimated convection, due to either biases in the sea-ice behaviour or in the ocean stratification.

From these results, we recommend changing a number of practices in ice-sheet projections:

– Several members within each climate model should be considered as forcing: given the number of degrees of freedom of climate models, it would probably be unrealistic to expect finding a member perfectly in phase with the observed variability among ensembles of a few tens of members, even if models were not biased, so it is important to account for this uncertainty.

– The reference period for the calculation of anomalies or weights should be longer than the 20 years used here and in ISMIP6 (Nowicki et al., 2020). Casado et al. (2023) recommend averaging over 50 years to be long enough to weaken internal climate variability and short enough not to dilute forced trends. An issue with extending the period over which the correction is applied is that only few observations were available 50 years ago in Antarctica, so it is possible that this approach will reduce the expression of internal climate variability in the model but not in the observations. This nonetheless likely remains a preferable approach than using the last 20 years.

– The initialisation of ice-sheet models should account for internal climate variability, either by starting from various members and/or by including internal climate variability in the long initialisation of some ice-sheet models, as previously suggested by Robel et al. (2023).

– Ice-sheet models should be fully coupled to climate models and be run for multiple members. Although still challenging (Smith et al., 2021), this would enable a consistent representation of internal climate variability, including the effects of ice-sheet–ocean and ice-sheet–atmosphere feedbacks.

Code and data availability. The ice-sheet model version and set of parameters used to run our experiments, the SMB reconstructions and the python scripts used to build the figures will be provided in a zenodo repository after the review.

Author contributions. JC and NCJ designed the overall study. JC wrote the initial draft and NCJ did the first review. JC ran the Elmer/Ice experiments with valuable inputs from PM, FGC, BU and MC. NCJ compiled the intercomparison of CMIP6 ocean models. NCJ, CA and CK calculated the multi-member surface mass balance. JC and CB worked on the basal melting parameterisation. All authors contributed to the final manuscript.

Competing interests. The authors declare no competing interests.

400

References

Adusumilli, S., Fricker, H. A., Medley, B., Padman, L., and Siegfried, M. R.: Interannual variations in meltwater input to the Southern Ocean from Antarctic ice shelves, Nature geoscience, 13, 616–620, 2020.

Agosta, C., Favier, V., Krinner, G., Gallée, H., Fettweis, X., and Genthon, C.: High-resolution modelling of the Antarctic surface mass balance, application for the twentieth, twenty first and twenty second centuries, Climate dynamics, 41, 3247–3260, 2013.

Agosta, C., Amory, C., Kittel, C., Orsi, A., Favier, V., Gallée, H., van den Broeke, M. R., Lenaerts, J., van Wessem, J. M., van de Berg, W. J., et al.: Estimation of the Antarctic surface mass balance using the regional climate model MAR (1979–2015) and identification of dominant processes, The Cryosphere, 13, 281–296, 2019.

Agosta, C., Kittel, C., Amory, C., Edwards, T., and Davrinche, C.: Evaluation of CMIP5 and CMIP6 global climate models in the Arctic and Antarctic regions, atmosphere and surface ocean, in: EGU General Assembly Conference Abstracts, pp. EGU22–11 363, 2022.

Armstrong McKay, D. I., Staal, A., Abrams, J. F., Winkelmann, R., Sakschewski, B., Loriani, S., Fetzer, I., Cornell, S. E., Rockström, J., and Lenton, T. M.: Exceeding 1.5 C global warming could trigger multiple climate tipping points, Science, 377, eabn7950, 2022.

Aschwanden, A., Bartholomaus, T. C., Brinkerhoff, D. J., and Truffer, M.: Brief communication: A roadmap towards credible projections of ice sheet contribution to sea level, The Cryosphere, 15, 5705–5715, 2021.

Beadling, R. L., Russell, J., Stouffer, R., Mazloff, M., Talley, L., Goodman, P., Sallée, J.-B., Hewitt, H., Hyder, P., and Pandde, A.: Representation of Southern Ocean properties across coupled model intercomparison project generations: CMIP3 to CMIP6, Journal of Climate, 33, 6555–6581, 2020.

Bindschadler, R. A., Nowicki, S., Abe-Ouchi, A., Aschwanden, A., Choi, H., Fastook, J., Granzow, G., Greve, R., Gutowski, G., Herzfeld, U., et al.: Ice-sheet model sensitivities to environmental forcing and their use in projecting future sea level (the SeaRISE project), Journal of Glaciology, 59, 195–224, 2013.

Boucher, O., Servonnat, J., Albright, A. L., Aumont, O., Balkanski, Y., Bastrikov, V., Bekki, S., Bonnet, R., Bony, S., Bopp, L., et al.: Presentation and evaluation of the IPSL-CM6A-LR climate model, J. Adv. Model. Ea. Sys., 12, e2019MS002 010, 2020.

Boyer, T. P., García, H. E., Locarnini, R. A., Zweng, M. M., Mishonov, A. V., Reagan, J. R., Weathers, K. A., Baranova, O. K., Paver, C. R., Seidov, D., et al.: World ocean atlas, 2018.

Brondex, J., Gillet-Chaulet, F., and Gagliardini, O.: Sensitivity of centennial mass loss projections of the Amundsen basin to the friction law, The Cryosphere, 13, 177–195, 2019.

Burgard, C., Jourdain, N. C., Reese, R., Jenkins, A., and Mathiot, P.: An assessment of basal melt parameterisations for Antarctic ice shelves, The Cryosphere, 16, 4931–4975, 2022.

Caillet, J., Jourdain, N. C., Mathiot, P., Hellmer, H. H., and Mouginot, J.: Drivers and reversibility of abrupt ocean state transitions in the Amundsen Sea, Antarctica, Journal of Geophysical Research: Oceans, 128, e2022JC018 929, 2023.

Casado, M., Hébert, R., Faranda, D., and Landais, A.: The quandary of detecting the signature of climate change in Antarctica, Nature Climate Change, pp. 1–7, 2023.

Cheung, A. H., Mann, M. E., Steinman, B. A., Frankcombe, L. M., England, M. H., and Miller, S. K.: Comparison of low-frequency internal climate variability in CMIP5 models and observations, Journal of Climate, 30, 4763–4776, 2017.

Comiso, J. C.: Bootstrap Sea Ice Concentrations from Nimbus-7 SMMR and DMSP SSM/I-SSMIS, Version 4, https://doi.org/10.5067/X5LG68MH013O, 2023.

Coulon, V., Klose, A. K., Kittel, C., Edwards, T., Turner, F., Winkelmann, R., and Pattyn, F.: Disentangling the drivers of future Antarctic ice loss with a historically-calibrated ice-sheet model, EGUsphere, 2023, 1–42, 2023.

Dalaiden, Q., Abram, N., and Goosse, H.: Tropical Pacific variability and anthropogenic forcing are the key drivers of the West Antarctic
440   atmospheric circulation variability over the 20th century, Tech. rep., Copernicus Meetings, 2023.

Donat-Magnin, M., Jourdain, N. C., Kittel, C., Agosta, C., Amory, C., Gallée, H., Krinner, G., and Chekki, M.: Future surface mass balance and surface melt in the Amundsen sector of the West Antarctic Ice Sheet, The Cryosphere, 15, 571–593, 2021.

Dutrieux, P., De Rydt, J., Jenkins, A., Holland, P. R., Ha, H. K., Lee, S. H., Steig, E. J., Ding, Q., Abrahamsen, E. P., and Schröder, M.: Strong sensitivity of Pine Island ice-shelf melting to climatic variability, Science, 343, 174–178, 2014.

445 Edwards, T. L., Nowicki, S., Marzeion, B., Hock, R., Goelzer, H., Seroussi, H., Jourdain, N. C., Slater, D. A., Turner, F. E., Smith, C. J., et al.: Projected land ice contributions to twenty-first-century sea level rise, Nature, 593, 74–82, 2021.

Eyring, V., Bony, S., Meehl, G. A., Senior, C. A., Stevens, B., Stouffer, R. J., and Taylor, K. E.: Overview of the Coupled Model Intercomparison Project Phase 6 (CMIP6) experimental design and organization, Geoscientific Model Development, 9, 1937–1958, 2016.

Fox-Kemper, B., Hewitt, H., Xiao, C., Aðalgeirsdóttir, G., Drijfhout, S. S., Edwards, T. L., Golledge, N. R., Hemer, M., Kopp, R. E., Krinner,
450   G., Mix, A., Notz, D., Nowicki, S., Nurhati, I. S., Ruiz, L., Sallée, J.-B., Slangen, A. B. A., and Yu, Y.: Ocean, Cryosphere and Sea Level Change, in: Climate Change 2021: The Physical Science Basis. Contribution of Working Group I to the Sixth Assessment Report of the Intergovernmental Panel on Climate Change, pp. 1211–1362, Cambridge University Press, Cambridge, United Kingdom and New York, NY, USA, https://doi.org/10.1017/9781009157896.011, 2021.

Gagliardini, O., Zwinger, T., Gillet-Chaulet, F., Durand, G., Favier, L., De Fleurian, B., Greve, R., Malinen, M., Martín, C., Råback, P., et al.:
455   Capabilities and performance of Elmer/Ice, a new-generation ice sheet model, Geoscientific Model Development, 6, 1299–1318, 2013.

Garbe, J., Albrecht, T., Levermann, A., Donges, J. F., and Winkelmann, R.: The hysteresis of the Antarctic ice sheet, Nature, 585, 538–544, 2020.

Genthon, C. and Cosme, E.: Intermittent signature of ENSO in west-Antarctic precipitation, Geophysical Research Letters, 30, 2003.

Gillet-Chaulet, F., Gagliardini, O., Seddik, H., Nodet, M., Durand, G., Ritz, C., Zwinger, T., Greve, R., and Vaughan, D. G.: Greenland ice
460   sheet contribution to sea-level rise from a new-generation ice-sheet model, The Cryosphere, 6, 1561–1576, 2012.

Glen, J. W.: The creep of polycrystalline ice, Proceedings of the Royal Society of London. Series A. Mathematical and Physical Sciences, 228, 519–538, 1955.

Goelzer, H., Coulon, V., Pattyn, F., De Boer, B., and Van De Wal, R.: Brief communication: On calculating the sea-level contribution in marine ice-sheet models, The Cryosphere, 14, 833–840, 2020.

465 Gwyther, D. E., O'Kane, T. J., Galton-Fenzi, B. K., Monselesan, D. P., and Greenbaum, J. S.: Intrinsic processes drive variability in basal melting of the Totten Glacier Ice Shelf, Nature communications, 9, 3141, 2018.

Henley, B. J., Gergis, J., Karoly, D. J., Power, S., Kennedy, J., and Folland, C. K.: A tripole index for the interdecadal Pacific oscillation, Climate dynamics, 45, 3077–3090, 2015.

Heuzé, C.: Antarctic bottom water and North Atlantic deep water in CMIP6 models, Ocean Science, 17, 59–90, 2021.

470 Hill, E. A., Urruty, B., Reese, R., Garbe, J., Gagliardini, O., Durand, G., Gillet-Chaulet, F., Gudmundsson, G. H., Winkelmann, R., Chekki, M., et al.: The stability of present-day Antarctic grounding lines–Part 1: No indication of marine ice sheet instability in the current geometry, The Cryosphere, 17, 3739–3759, 2023.

Hirano, D., Tamura, T., Kusahara, K., Fujii, M., Yamazaki, K., Nakayama, Y., Ono, K., Itaki, T., Aoyama, Y., Simizu, D., et al.: On-shelf circulation of warm water toward the Totten Ice Shelf in East Antarctica, Nature Communications, 14, 4955, 2023.

475   Hogg, A. M., Penduff, T., Close, S. E., Dewar, W. K., Constantinou, N. C., and Martínez-Moreno, J.: Circumpolar variations in the chaotic
nature of Southern Ocean eddy dynamics, Journal of Geophysical Research: Oceans, 127, e2022JC018 440, 2022.

Holland, P. R., Bracegirdle, T. J., Dutrieux, P., Jenkins, A., and Steig, E. J.: West Antarctic ice loss influenced by internal climate variability
and anthropogenic forcing, Nature Geoscience, 12, 718–724, 2019.

Holland, P. R., O'Connor, G. K., Bracegirdle, T. J., Dutrieux, P., Naughten, K. A., Steig, E. J., Schneider, D. P., Jenkins, A., and Smith, J. A.:

480   Anthropogenic and internal drivers of wind changes over the Amundsen Sea, West Antarctica, during the 20th and 21st centuries, The
Cryosphere, 16, 5085–5105, 2022.

Jenkins, A., Shoosmith, D., Dutrieux, P., Jacobs, S., Kim, T. W., Lee, S. H., Ha, H. K., and Stammerjohn, S.: West Antarctic Ice Sheet retreat
in the Amundsen Sea driven by decadal oceanic variability, Nature Geoscience, 11, 733–738, 2018.

Jourdain, N. C., Asay-Davis, X., Hattermann, T., Straneo, F., Seroussi, H., Little, C. M., and Nowicki, S.: A protocol for calculating basal

485   melt rates in the ISMIP6 Antarctic ice sheet projections, The Cryosphere, 14, 3111–3134, 2020.

Jourdain, N. C., Amory, C., Kittel, C., and Durand, G.: Changes in Antarctic surface conditions and potential for ice shelf hydrofracturing
from 1850 to 2200, The Cryosphere, submitted, 2024.

Kittel, C., Amory, C., Agosta, C., Jourdain, N. C., Hofer, S., Delhasse, A., Doutreloup, S., Huot, P.-V., Lang, C., Fichefet, T., et al.: Diverging
future surface mass balance between the Antarctic ice shelves and grounded ice sheet, The Cryosphere, 15, 1215–1236, 2021.

490   Kittel, C., Amory, C., Hofer, S., Agosta, C., Jourdain, N. C., Gilbert, E., Le Toumelin, L., Vignon, É., Gallée, H., and Fettweis, X.: Clouds
drive differences in future surface melt over the Antarctic ice shelves, The Cryosphere, 16, 2655–2669, 2022.

Kravtsov, S., Dewar, W. K., Berloff, P., McWilliams, J. C., and Ghil, M.: A highly nonlinear coupled mode of decadal variability in a
mid-latitude ocean–atmosphere model, Dynamics of atmospheres and oceans, 43, 123–150, 2007.

Krinner, G., Guicherd, B., Ox, K., Genthon, C., and Magand, O.: Influence of oceanic boundary conditions in simulations of Antarctic climate

495   and surface mass balance change during the coming century, Journal of Climate, 21, 938–962, 2008.

Lee, J.-Y., Dunne, J. P., Engelbrecht, F., Fischer, E., Fyfe, J. C., Jones, C., A., M., Mutemi, J., Ndiaye, O., Panickal, S., and Zhou, T.:
Chapter 4: Future global climate: scenario-based projections and near-term information, in: Climate Change 2021: The Physical Science
Basis. Contribution of Working Group I to the Sixth Assessment Report of the Intergovernmental Panel on Climate Change, pp. 553–672,
[Masson-Delmotte,V., P. Zhai,A. Pirani, S.L. Connors, C. Péan, S. Berger, N. Caud,Y. Chen, L. Goldfarb, M.I. Gomis, M. Huang, K.

500   Leitzell, E. Lonnoy, J.B.R. Matthews, T.K. Maycock, T. Waterfield, O. Yelekçi, R. Yu, and B. Zhou (eds.)]. Cambridge University Press,
Cambridge, United Kingdom and New York, NY, USA, 2021.

MacAyeal, D. R.: Large-scale ice flow over a viscous basal sediment: Theory and application to ice stream B, Antarctica, Journal of Geo-
physical Research: Solid Earth, 94, 4071–4087, 1989.

Marshall, G. J.: Trends in the Southern Annular Mode from observations and reanalyses, Journal of climate, 16, 4134–4143, 2003.

505   Marshall, G. J. and Thompson, D. W.: The signatures of large-scale patterns of atmospheric variability in Antarctic surface temperatures,
Journal of Geophysical Research: Atmospheres, 121, 3276–3289, 2016.

Mathiot, P. and Jourdain, N. C.: Southern Ocean warming and Antarctic ice shelf melting in conditions plausible by late 23rd century in a
high-end scenario, Ocean Sciecne, 0, 1–27, 2023.

Mathiot, P., Jenkins, A., Harris, C., and Madec, G.: Explicit and parametrised representation of under ice shelf seas in az* coordinate ocean

510   model NEMO 3.6, Geosci. Model Dev., 10, 2849–2874, 2017.

Medley, B. and Thomas, E.: Increased snowfall over the Antarctic Ice Sheet mitigated twentieth-century sea-level rise, Nature Climate
Change, 9, 34–39, 2019.

Meehl, G. A., Senior, C. A., Eyring, V., Flato, G., Lamarque, J.-F., Stouffer, R. J., Taylor, K. E., and Schlund, M.: Context for interpreting equilibrium climate sensitivity and transient climate response from the CMIP6 Earth system models, Science Advances, 6, eaba1981,
515   2020.

Meier, W. N., Stewart, J. S., Windnagel, A., and Fetterer, F. M.: Comparison of hemispheric and regional sea ice extent and area trends from NOAA and NASA passive microwave-derived climate records, Remote Sensing, 14, 619, 2022.

Morlighem, M., Rignot, E., Binder, T., Blankenship, D., Drews, R., Eagles, G., Eisen, O., Ferraccioli, F., Forsberg, R., Fretwell, P., et al.: Deep glacial troughs and stabilizing ridges unveiled beneath the margins of the Antarctic ice sheet, Nature Geoscience, 13, 132–137, 2020.

520   Mottram, R., Hansen, N., Kittel, C., van Wessem, J. M., Agosta, C., Amory, C., Boberg, F., van de Berg, W. J., Fettweis, X., Gossart, A., et al.: What is the surface mass balance of Antarctica? An intercomparison of regional climate model estimates, The Cryosphere, 15, 3751–3784, 2021.

Mouginot, J., Rignot, E., and Scheuchl, B.: Continent-wide, interferometric SAR phase, mapping of Antarctic ice velocity, Geophysical Research Letters, 46, 9710–9718, 2019.

525   Müller, W. A., Jungclaus, J. H., Mauritsen, T., Baehr, J., Bittner, M., Budich, R., Bunzel, F., Esch, M., Ghosh, R., Haak, H., et al.: A higher-resolution version of the max planck institute earth system model (MPI-ESM1. 2-HR), J. Adv. Model. Ea. Sys., 10, 1383–1413, 2018.

Naughten, K. A., Holland, P. R., and De Rydt, J.: Unavoidable future increase in West Antarctic ice-shelf melting over the twenty-first century, Nature Climate Change, pp. 1–7, 2023.

530   Nowicki, S., Goelzer, H., Seroussi, H., Payne, A. J., Lipscomb, W. H., Abe-Ouchi, A., Agosta, C., Alexander, P., Asay-Davis, X. S., Barthel, A., et al.: Experimental protocol for sea level projections from ISMIP6 stand-alone ice sheet models, The Cryosphere, 14, 2331–2368, 2020.

Parsons, L. A., Brennan, M. K., Wills, R. C., and Proistosescu, C.: Magnitudes and spatial patterns of interdecadal temperature variability in CMIP6, Geophysical Research Letters, 47, e2019GL086 588, 2020.

535   Payne, A. J., Nowicki, S., Abe-Ouchi, A., Agosta, C., Alexander, P., Albrecht, T., Asay-Davis, X., Aschwanden, A., Barthel, A., Bracegirdle, T. J., et al.: Future sea level change under coupled model intercomparison project phase 5 and phase 6 scenarios from the Greenland and Antarctic ice sheets, Geophysical Research Letters, 48, e2020GL091 741, 2021.

Penduff, T., Sérazin, G., Leroux, S., Close, S., Molines, J.-M., Barnier, B., Bessières, L., Terray, L., and Maze, G.: Chaotic variability of ocean heat content: climate-relevant features and observational implications, Oceanography, 31, 63–71, 2018.

540   Previdi, M. and Polvani, L. M.: Anthropogenic impact on Antarctic surface mass balance, currently masked by natural variability, to emerge by mid-century, Environmental Research Letters, 11, 094 001, 2016.

Purich, A. and England, M. H.: Historical and future projected warming of Antarctic Shelf Bottom Water in CMIP6 models, Geophysical Research Letters, 48, e2021GL092 752, 2021.

Reese, R., Albrecht, T., Mengel, M., Asay-Davis, X., and Winkelmann, R.: Antarctic sub-shelf melt rates via PICO, The Cryosphere, 12,
545   1969–1985, 2018.

Reese, R., Garbe, J., Hill, E. A., Urruty, B., Naughten, K. A., Gagliardini, O., Durand, G., Gillet-Chaulet, F., Gudmundsson, G. H., Chandler, D., et al.: The stability of present-day Antarctic grounding lines–Part 2: Onset of irreversible retreat of Amundsen Sea glaciers under current climate on centennial timescales cannot be excluded, The Cryosphere, 17, 3761–3783, 2023.

Rignot, E., Jacobs, S., Mouginot, J., and Scheuchl, B.: Ice-shelf melting around Antarctica, Science, 341, 266–270, 2013.

550 Rignot, E., Mouginot, J., Scheuchl, B., Van Den Broeke, M., Van Wessem, M. J., and Morlighem, M.: Four decades of Antarctic Ice Sheet mass balance from 1979–2017, Proceedings of the National Academy of Sciences, 116, 1095–1103, 2019.

Robel, A., Verjans, V., and Ambelorun, A.: Biases in ice sheet models from missing noise-induced drift, EGUsphere, 2023, 1–14, 2023.

Scott, R. C., Nicolas, J. P., Bromwich, D. H., Norris, J. R., and Lubin, D.: Meteorological drivers and large-scale climate forcing of West Antarctic surface melt, Journal of Climate, 32, 665–684, 2019.

555 Sellar, A. A., Walton, J., Jones, C. G., Wood, R., Abraham, N. L., Andrejczuk, M., Andrews, M. B., Andrews, T., Archibald, A. T., de Mora, L., et al.: Implementation of UK Earth system models for CMIP6, J. Adv. Model. Ea. Sys., 12, e2019MS001 946, 2020.

Sérazin, G., Jaymond, A., Leroux, S., Penduff, T., Bessières, L., Llovel, W., Barnier, B., Molines, J.-M., and Terray, L.: A global probabilistic study of the ocean heat content low-frequency variability: Atmospheric forcing versus oceanic chaos, Geophysical Research Letters, 44, 5580–5589, 2017.

560 Seroussi, H., Morlighem, M., Larour, E., Rignot, E., and Khazendar, A.: Hydrostatic grounding line parameterization in ice sheet models, The Cryosphere, 8, 2075–2087, 2014.

Seroussi, H., Nowicki, S., Payne, A. J., Goelzer, H., Lipscomb, W. H., Abe-Ouchi, A., Agosta, C., Albrecht, T., Asay-Davis, X., Barthel, A., et al.: ISMIP6 Antarctica: a multi-model ensemble of the Antarctic ice sheet evolution over the 21st century, The Cryosphere, 14, 3033–3070, 2020.

565 Seroussi, H., Verjans, V., Nowicki, S., Payne, A. J., Goelzer, H., Lipscomb, W. H., Abe Ouchi, A., Agosta, C., Albrecht, T., Asay-Davis, X., et al.: Insights on the vulnerability of Antarctic glaciers from the ISMIP6 ice sheet model ensemble and associated uncertainty, The Cryosphere Discussions, 2023, 1–28, 2023.

Shepherd, A., Gilbert, L., Muir, A. S., Konrad, H., McMillan, M., Slater, T., Briggs, K. H., Sundal, A. V., Hogg, A. E., and Engdahl, M. E.: Trends in Antarctic Ice Sheet elevation and mass, Geophysical Research Letters, 46, 8174–8183, 2019.

570 Siahaan, A., Smith, R. S., Holland, P. R., Jenkins, A., Gregory, J. M., Lee, V., Mathiot, P., Payne, A. J., Ridley, J. K., and Jones, C. G.: The Antarctic contribution to 21st-century sea-level rise predicted by the UK Earth System Model with an interactive ice sheet, The Cryosphere, 16, 4053–4086, 2022.

Silvano, A., Holland, P. R., Naughten, K. A., Dragomir, O., Dutrieux, P., Jenkins, A., Si, Y., Stewart, A. L., Peña Molino, B., Janzing, G. W., et al.: Baroclinic Ocean Response to Climate Forcing Regulates Decadal Variability of Ice-Shelf Melting in the Amundsen Sea, 575 Geophysical Research Letters, 49, e2022GL100 646, 2022.

Smith, J. A., Andersen, T. J., Shortt, M., Gaffney, A. M., Truffer, M., Stanton, T. P., Bindschadler, R., Dutrieux, P., Jenkins, A., Hillenbrand, C. D., Ehrmann, W., Corr, H. F., Farley, N., Crowhurst, S., and Vaughan, D. G.: Sub-ice-shelf sediments record history of twentieth-century retreat of Pine Island Glacier, Nature, 541, https://doi.org/10.1038/nature20136, 2017.

Smith, R. S., Mathiot, P., Siahaan, A., Lee, V., Cornford, S. L., Gregory, J. M., Payne, A. J., Jenkins, A., Holland, P. R., Ridley, J. K., et al.: 580 Coupling the UK Earth System Model to dynamic models of the Greenland and Antarctic ice sheets, Journal of Advances in Modeling Earth Systems, 13, e2021MS002 520, 2021.

Steig, E. J., Ding, Q., Battisti, D., and Jenkins, A.: Tropical forcing of Circumpolar Deep Water inflow and outlet glacier thinning in the Amundsen Sea Embayment, West Antarctica, Annals of Glaciology, 53, 19–28, 2012.

The IMBIE Team: Mass balance of the Antarctic Ice Sheet from 1992 to 2017, Nature, 558, 219–222, https://doi.org/10.1038/s41586-018-585 0179-y, 2018.

Tsai, C.-Y., Forest, C. E., and Pollard, D.: The role of internal climate variability in projecting Antarctica's contribution to future sea-level rise, Climate dynamics, 55, 1875–1892, 2020.

Van Wessem, J. M., Van De Berg, W. J., Noël, B. P., Van Meijgaard, E., Amory, C., Birnbaum, G., Jakobs, C. L., Krüger, K., Lenaerts, J. T.,
    Lhermitte, S., et al.: Modelling the climate and surface mass balance of polar ice sheets using RACMO2–Part 2: Antarctica (1979–2016),
590   The Cryosphere, 12, 1479–1498, 2018.

Verfaillie, D., Pelletier, C., Goosse, H., Jourdain, N. C., Bull, C. Y., Dalaiden, Q., Favier, V., Fichefet, T., and Wille, J. D.: The circum-
    Antarctic ice-shelves respond to a more positive Southern Annular Mode with regionally varied melting, Communications Earth & Envi-
    ronment, 3, 139, 2022.

Wang, Y., Yuan, X., and Cane, M. A.: Coupled mode of cloud, atmospheric circulation, and sea ice controlled by wave-3 pattern in Antarctic
595   winter, Environmental Research Letters, 17, 044 053, 2022.

Williams, G., Herraiz-Borreguero, L., Roquet, F., Tamura, T., Ohshima, K., Fukamachi, Y., Fraser, A., Gao, L., Chen, H., McMahon, C.,
    et al.: The suppression of Antarctic bottom water formation by melting ice shelves in Prydz Bay, Nature communications, 7, 12 577, 2016.

Zhang, L., Delworth, T. L., Cooke, W., and Yang, X.: Natural variability of Southern Ocean convection as a driver of observed climate trends,
    Nature Climate Change, 9, 59–65, 2019.